Supplementary Material

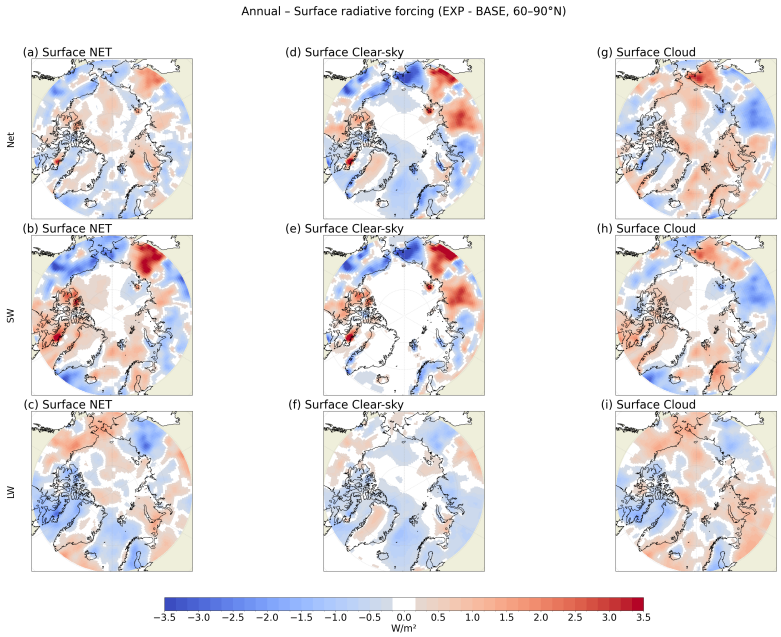

Figure S1: Differences in annual mean surface radiative flux components between the blowing-snow simulation and the control run. Panels show (a) surface net flux, (b) net shortwave (SW), (c) net longwave (LW), (d) net clear-sky flux, (e) clear-sky SW, (f) clear-sky LW, (g) net cloud radiative effect, (h) cloud SW effect, and (i) cloud LW effect. Positive values indicate increased downward flux relative to the reference simulation, and negative values indicate a reduction in surface radiative input.

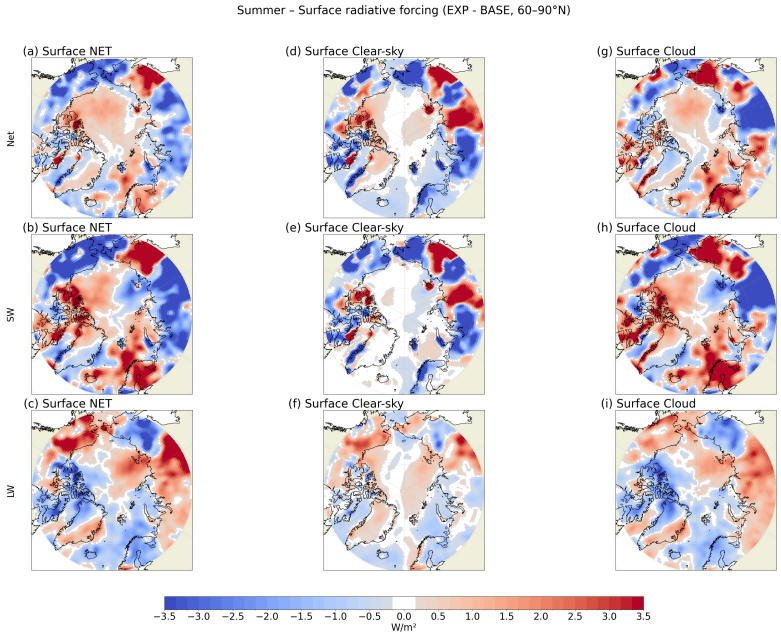

Figure S2: Same as S1 but for JJA

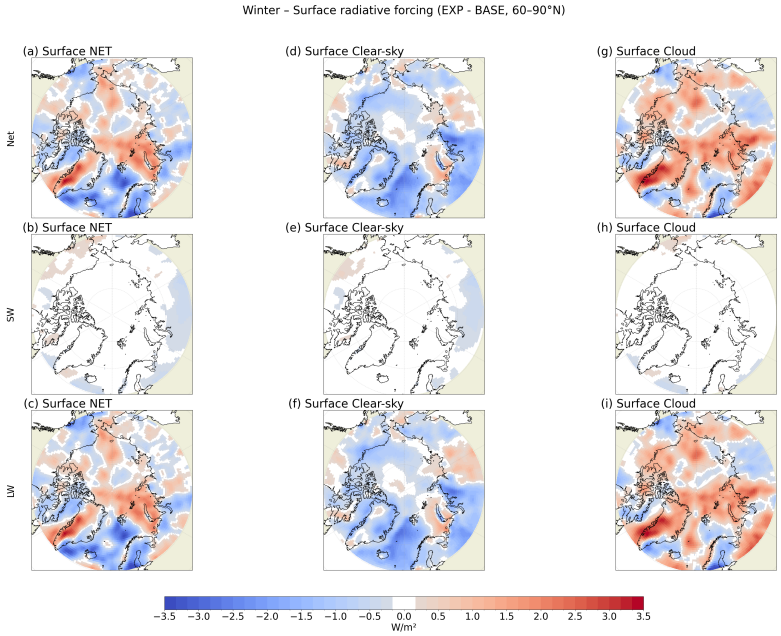

Figure S3: Same as S1 but for DJF

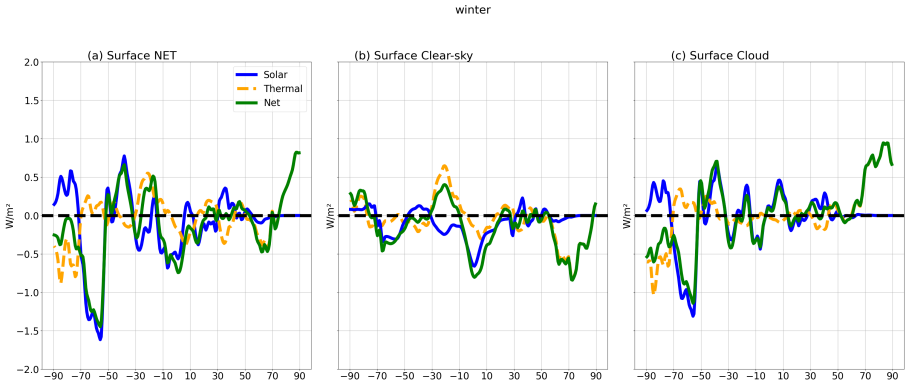

Figure S4: Same as fig 8 but for DJF

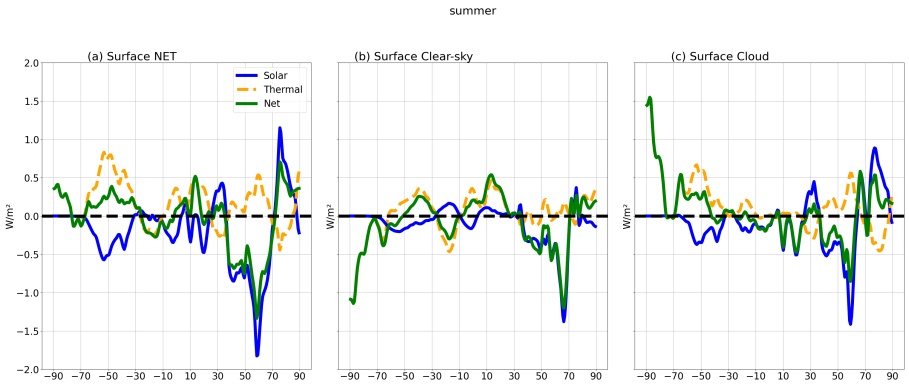

Figure S5: Same as fig8 but for JJA

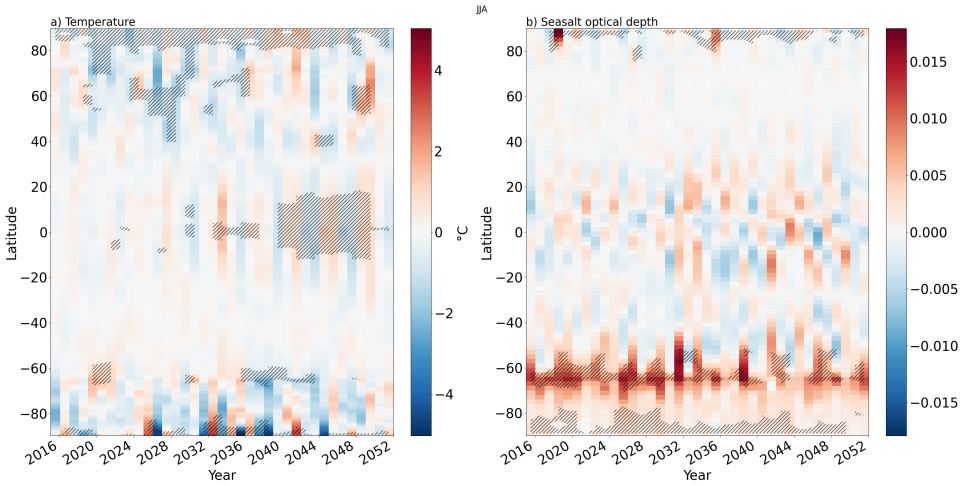

Figure S6: Zonal-mean June–July–August (JJA) response to the inclusion of the blowing-snow parameterization. (a) Zonal-mean temperature differences (blowing-snow minus reference simulation) averaged over JJA. (b) Corresponding zonal-mean sea-salt AOD differences for JJA. In both panels, stippling denotes regions where the differences are statistically significant at the $p < 0.05$ level. The summertime response is generally weak, consistent with the limited radiative impact of additional sea-salt scattering during JJA and reduced blowing-snow activity. Differences are computed relative to the reference simulation without the blowing-snow parameterization.

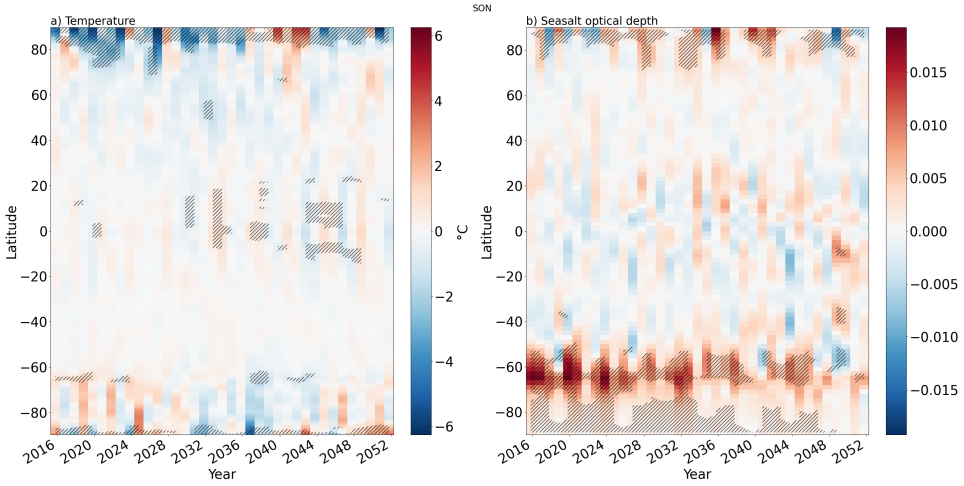

Figure S7: Same as S6, for SON

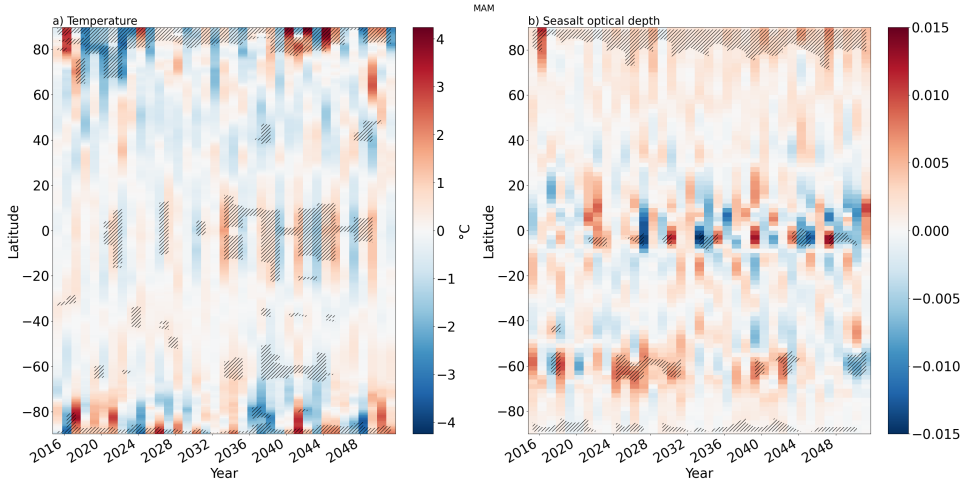

Figure S8: Same as S6, for MAM

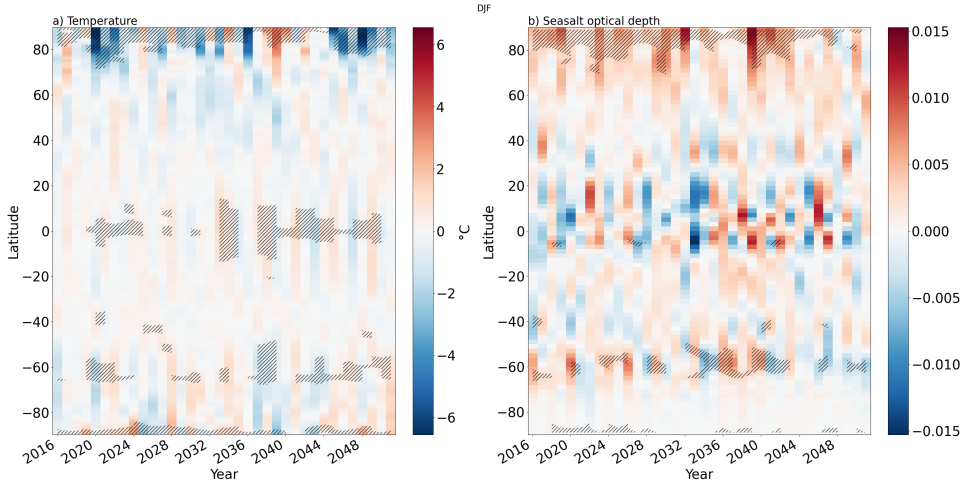

Figure S9: Same as S6, for DJF